ACCURACY INVESTIGATION ON LARGE BLOCKS OF HIGH RESOLUTION IMAGES

Ricardo M. Passini (*),Karsten Jacobsen (**)
(*) BAE SYSTEMS, rpassini@adrinc.com;
(**) University of Hannover, jacobsen@ipi.uni-hannover.de

Keywords: QuickBird, Scene Orientation, Block Adjustment, Quaternion, ephemeris, Rational Polynomial Coefficients

ABSTRACT:

A large block of QuickBird Basic Imagery has been analyzed for optimal control distribution and scene ties. This has been done by three dimensional adjustment of a block of Basic Imagery using satellite ephemeris and attitude (quaternion) data along with ground control points (GCPs). Different GCPs configuration and check points were used to assess the achieved accuracy. Only the horizontal coordinates of the ground control points and check points have been available, so the SRTM – height model was used for the third dimension. Discrepancies between the inner and exterior accuracy determined by check points indicate remaining systematic effects of the QuickBird images. Recommendations for the handling and the control point density are given.

1. INTRODUCTION

Digital Orthophotos is the most commonly and widely used mapping product in these days. The processes involved for its generation have been highly automated to a large degree what makes a very economically attractive alternative to the traditional line mapping. It has all the metric characteristics of map plus the wealth of pictorial information. It requires a direct reading with almost no interpretation as it is necessary in a vector mapping. In other words the cartographic symbols are replaced by the image of the same features.

Most modern high resolution optical satellites allow the simultaneous acquisition of color and panchromatic bands as well as the exposition or large coverage in a almost continuous mode.

The accuracy of the image orientation parameters and the digital terrain model are of paramount importance for a successful orthophoto project. The number and distribution of GCPs along with the orientation model are the key factor for the accuracy of the orientation parameters. The present investigation concentrates on the study of the Orientation Accuracy using mainly two orientation methods and different number and distribution of ground control points (GCPs). For that purpose a block of high resolution B/W panchromatic band QuickBird images was used. It is composed of 40 images from 6 contiguous orbits. GCPs were manually transferred from higher resolution and accurate stereoscopically oriented panchromatic imagery. Orientation accuracies of the original imagery relative to check points in the range of around 1.0 meter have been reported. Figure 1 shows the block along with the GCP distribution.

In relation to the used Orientation Models, two were employed, namely the Space Resection based on the Satellite Ephemeris and on the Attitude Quaternion; and a second based on enhanced Rational Polynomial Coefficients. The Observations were made using the Socet Set Systems through its Multi-Sensor Triangulation (MST) module.

2. ORIENTATION MODELS

2.1. Bundle Orientation with Self-Calibration

The Bundle Model is based on the widely known co-linearity condition equation of line scanner array of CCD elements:

$$0 = -c\frac{a_{11}^{\,j}(Xp - Xo^{j}) + a_{12}^{\,j}(Yp - Yo^{j}) + a_{13}^{\,j}(Zp - Zo^{j})}{a_{31}^{\,j}(Xp - Xo^{j}) + a_{32}^{\,j}(Yp - Yo^{j}) + a_{33}^{\,j}(Zp - Zo^{j})} + add\ param$$

$$y = -c\frac{a_{21}^{\,j}(Xp - Xo^{j}) + a_{22}^{\,j}(Yp - Yo^{j}) + a_{23}^{\,j}(Zp - Zo^{j})}{a_{31}^{\,j}(Xp - Xo^{j}) + a_{32}^{\,j}(Yp - Yo^{j}) + a_{33}^{\,j}(Zp - Zo^{j})} + add\ param$$

With: Xo^{j} , Yo^{j} : projection center coordinates for the image line j

Xp, Yp, Zp: ground coordinates of the object point p

$a_{i,k}{}^{1j}$; i, k=1, 2, 3: elements of the rotation matrix for the line image j

$0, y_p$: image coordinates of image point p

formula 1: collinearity equation for CCD-line scanner images

The exterior orientation parameters of each image line are different, but the relationship of the exterior orientation to the satellite orbit is only changing slightly. Hence for the classical CCD-line cameras, the attitudes are only changing slightly in relation to the satellite orbit, for an image it is possible to consider time (space) dependent attitude parameters. Taking into consideration the general information about the view direction of the satellite, the "in track and across track view angles" (included within the QuickBird *.imd-file) and knowing that in a Basic Imagery the

effects of the high frequency movements have been eliminated, then the effects of the low frequency motions of the platform can be modeled by self calibration via additional parameters.
The additional parameters been used by the Hannover orientation program BLASPO are checked for numerical stability, statistical significance and reliability in order to justify their presence and to avoid over-parameterization. The program automatically reduces the additional parameters specified by dialogue to the required group of images by a statistical analysis based on a combination of Student-test, the correlation and total correlation. This guarantees that no over-parameterization occurs. In that case an extrapolation outside the area covered by control points does not become dangerous.

The elimination process is as follows:
1. For each additional parameter compute:

$t_i = \frac{|p_i|}{\sigma_{pi}}$; $\sigma_{pi} = \sqrt{q_{ii}} \cdot \sigma_o$, $t_i \geq 1$, reject if otherwise

2. Compute cross-correlation coefficients for the parameters

$R_{ij} = \frac{q_{ij}}{\sqrt{q_{ii} \cdot q_{jj}}}$ $R_{ij} \geq 0.85$ then eliminate the parameter with smaller t_i value

3. Compute B = I – (diag N * diag $N^{-1})^{-1}$, eliminate the additional parameter with $B_{ii} \geq 0.85$

formula 2: strategy against over-parameterization

2.2 Bundle Orientation using Ephemeris and Attitude Quaternion

The Camera Sensor Model distributed by DigitalGlobe contains five coordinates systems, namely:
Earth Coordinates (E), Spacecraft Coordinates (S), Camera Coordinates (C), Detector Coordinates (D) and Image Coordinates (I),. Definitions and details regarding these systems can be found in DigitalGlobe QuickBird Imagery Products, Product Guide.
The data contained in the Ephemeris File and in the Attitude File are sample mean and covariance estimates of the position and attitude of the spacecraft system relative to the ECEF system. These data are produced for a continuous image period, e.g., an image or strip, and span the period from at least four seconds before start of imaging to at least four seconds after the end of imaging.
The instantaneous spacecraft attitude is represented by four-element quaternion. It describes a hypothetical 3D rotation of the spacecraft frame with respect to the ECEF frame. Any such a 3D rotation can be expressed by a rotation angle, θ, and an axis of rotation given by unit vector components (ε_x, ε_y, ε_z) in the ECEF frame. The sign and rotation angle follows the right-hand rule. Finally the quaternion (q1, q2, q3, q4) is related to θ and by (ε_x, ε_y, ε_z):

q1 = $\varepsilon_x \sin(\theta/2)$
q2 = $\varepsilon_y \sin(\theta/2)$
q3 = $\varepsilon_z \sin(\theta/2)$
q4=$\cos(\theta/2)$

formula 3: quaernion

Using quaternion algebra it is possible to transform a vector from the image domain into the ECEF coordinate system through:

$\mathbf{w}_E = \mathbf{q}^E_S(t)^{-1} \mathbf{q}^S_C{}^{-1} \mathbf{w}_C \mathbf{q}^S_C \mathbf{q}^E_S(t)$ or
$\mathbf{w}_E = \mathbf{q}^S_E(t) \mathbf{q}^C_S \mathbf{w}_C (\mathbf{q}^S_E(t) \mathbf{q}^C_S)^{-1}$ or using matrix algebra, $\mathbf{w}_E = \mathbf{R}^E_S(t) \mathbf{R}^S_C \mathbf{w}_C$
formula 4: transformation with quaternion

The resulting multiplication matrix $R^E_C(t)$ has following form:

$$[R^E_C(t)]^T = (\mathbf{R}^E_S(t)\mathbf{R}^S_C)^T =$$

$$\frac{1}{\omega^2+a_{(t)}^2+b_{(t)}^2+c_{(t)}^2} \begin{bmatrix} \omega^2+a_{(t)}^2-b_{(t)}^2-c_{(t)}^2 & 2a_{(t)}b_{(t)}+2\omega c_{(t)} & 2a_{(t)}c_{(t)}-2\omega b_{(t)} \\ 2a_{(t)}b_{(t)}-2\omega c_{(t)} & \omega^2-a_{(t)}^2+b_{(t)}^2-c_{(t)}^2 & 2b_{(t)}c_{(t)}+2\omega a_{(t)} \\ 2b_{(t)}c_{(t)}+2\omega b_{(t)} & 2b_{(t)}c_{(t)}-2\omega a_{(t)} & \omega^2-a_{(t)}^2-b_{(t)}^2+c_{(t)}^2 \end{bmatrix}$$

With: w_C = Vector in the image domain
(t): Time t (corresponding to exposed line j)
q^C_S w_C (q^S_E (t) = Vector in the Spacecraft coordinate system
$q^S_E(t)$ q^C_S w_C (q^S_E (t) $q^C_S)^{-1}$ = Vector in the ECEF coordinate system
$R^E_S(t)$ R^S_C = $R^E_C(t)$ = $(R^E_S(t)R^S_C)^T$= Rotation Matrix camera – ECEF coordinates systems at time t
ω = constant term, being a function of both scalars $\mathbf{q}^E_S$ **(4)** and $\mathbf{q}^S_C$ **(4)**
$a_{(t)}$; $b_{(t)}$; $c_{(t)}$= elements of the instantaneous rotation matrix $[R^E_C(t)]^T$ also function of the quaternion $\mathbf{q}^E_S(t)$ for the instant (t) and $\mathbf{q}^C_S$. formula 5 can in this way be used in the bundle orientation.
formula 5: transformed quaternion

One of the advantages of using the quaternion–ephemeris data along with their supplied statistics is the possibility of using a weighting scheme for each observed point in the image space.

$$W^j_k = \left(\Sigma^j_k\right)^{-1}$$

With: W^j_k = Weight associated with the point k on image j
Σ^j_k = Variance-covariance estimates for the quaternions and position ephemeris associated with the point k in image j
formula 6: weight function

2.3 Block Adjustment based on Rational Polynomial Coefficients (RPC)

The Rational Polynomial Coefficients (RPC) model relates the object space coordinates (φ, λ, h) to the image space coordinates system (*Line, Sample*). The RPC model is represented by a ratio of two cubic polynomials of object space coordinates. Two different ratios of cubic functions are used to express the image coordinates as function of the object coordinates. Image and object space coordinates are normalized between -1 and +1 to improve accuracy and to avoid memory overflow.

The normalized ellipsoidal latitude, longitude and height over the ellipsoid can be expressed by:

$$P = \frac{\varphi - \text{LAT\_OFF}}{\text{LAT\_SCALE}} \qquad L = \frac{\lambda - LONG\_OFF}{LONG\_SCALE}$$

$$H = \frac{h - HEIGHT\_OFF}{HEIGHT\_SCALE}$$

With*: LAT_OFF; LONG_OFF; HEIGHT_OFF* as latitude, longitude and height offsets

LAT_SCALE; LONG_SCALE; HEIGHT_SCALE as latitude, longitude and height scale

formula 7: normalized object coordinates

The normalized computed *Line* and *Sample* of the point in question in the image space are:

$$Y = Line = g(\varphi, \lambda, h) = \frac{NUM_L(P,L,H)}{DEN_L(P,L,H)}$$

$$X = Sample = h(\varphi,\lambda,h) = \frac{NUM_S(P,L,H)}{DEN_S(P,L,H)}$$

Where: NUM_L and DEN_S are

$$Pn(P,L,H)j = a_1 + a_2*L + a_3*P + a_4*H + a_5*L*P + a_6*L*H + a_7*P*H + a_8*L^2 + a_9*P^2 + a_{10}*H^2 + a_{11}*L*P*H + a_{12}*L^3 + a_{13}*L*P^2 + a_{14}*L*H^2 + a_{15}*L^2*P + a_{16}*P^3 + a_{17}*P*H^2 + a_{18}*L^2*H + a_{19}*P^2*H + a_{20}*H^3$$

with $Line = Y * LINE\_SCALE + LINE\_OFF$

$$Sample = X * SAMP\_SCALE + SAMP\_OFF$$

formula 8: RPCs

The RPCsare derived from a 3D grid generated using the physical camera model and the collected and recorded orbital data such as the ephemeris and attitude data. These, as any recorded statistics contains errors (ephemeris errors, attitude errors, drifts errors), whose effects are strongly correlated with others sources. It can be shown that in high resolution satellites, due to the narrow instantaneous field of view (IFOV) the in-track and across-track position errors are almost totally correlated with pitch and roll attitude errors, hence they can not be separately estimated. On the other hand, due to the relatively small swath the yaw errors are insignificant when compared to the other attitude errors. Hence, pitch and roll are the only attitude parameters to be estimated precisely.

Effects of attitude errors are highly systematic (biases), but there is a strong possibility that these errors may drift with the time. The attitude data are originated on star sensors and gyros. Errors in these can be accumulated on time if they cannot be compensated by other external information. In the case of the IKONOS images, these errors were shown to be small (i.e., less than a few pixels over 100 Km; (Grodecki 2001, Grodecki, Dial 2003).

$$Line_i^{(j)} = \xi^{(j)}(\varphi_s, \lambda_s, h_s) + d\xi^{(j)} + \nabla_{Li}$$

$$Sample_i^{(j)} = \rho^{(j)}(\varphi_s, \lambda_s, h_s) + d\rho^{(j)} + \nabla_{Si}$$

formula 9: bias correction of RPC solution

The effects of all above errors are noticeable in the difference between the computed and the observed image coordinates. Hence, additional parameters should be add to the computed line and sample to model such difference. In this respect the model proposed by Grodecki 2001, Grodecki, Dial 2003 will be tested for the QuickBird image block.

3. Experimental Tests

3.1 Colinearity model with additional parameters

The orientation model based on colinearity equations and additional parameters was tested using a QuickBird Basic B/W Panchromatic Image covering the area of Atlantic City (NJ). Ground control was transferred from existing digital orthophotos at 50 cm resolution GSD and a DTM of 30 cm vertical standard deviation. 382 common points between the ortho-images and the QuickBird were correlated matched and transferred.

			GCPs		Check Points	
Type	No. GCPs	σ_o [µm]	RMSX [m]	RMSY [m]	RMSX [m]	RMSY [m]
Manual	174	14.6	0.85	0.64		
Automatic	398	11.4	0.55	0.64		
Automatic	25	14.1	0.49	0.74	0.69	0.72
Automatic	20	13.4	0.53	0.56	0.69	1.39
Automatic	15	19.0	0.54	0.96	0.78	1.38

table 1: Root mean square discrepancy at GCPs and check points - Atlantic City, NJ

Firstly 174 GCPs have been measured manually; later 398 GCPs were determined by automatic matching of the reference orthophotos with the QuickBird scene by Socet Set. The achieved accuracy of the automatically matched points is better than the accuracy of the manual measured points.

The positioning is reaching approximately 1 pixel – this seam to be an operational result. Nevertheless, we notice that with smaller number of GCPs, the discrepancies at check points are becoming larger, but this can partially be explained by the control point quality itself and by the fact that with smaller number of GCPs the reliability of the determination of the values of the additional parameters becomes lower and consequently the standard deviation becomes larger (see table 1).

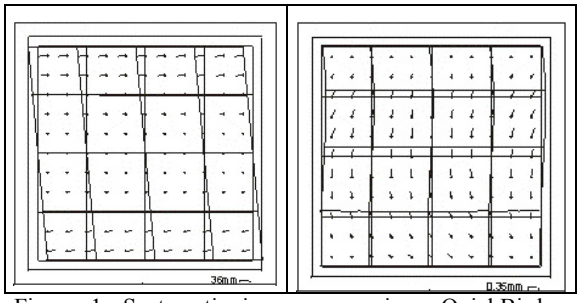

Figure 1: Systematic image errors in a QuickBird image of Atlantic City

As it can be seen in the left hand side of figure 1, the influence of the yaw control to the scene is covered by the additional parameters. This is reaching and angular affinity in the order of 12.5°. The non linear effect on the right hand side of figure 1 shows the low attitude frequencies to the scene. These are also being removed by the included additional parameters and tested for over-parameterization based on the statistical procedures explained above.

3.2. Block Adjustment using Ephemeris and Attitude Quaternion

Figure 2 shows the foot print of the block of QuickBird images along with the location of the maximal used 89 GCPs (case A). Case B is a perimeter control configuration with few GCPs in the center (figure 3) while case C has only perimeter control. Case D has relaxed perimeter control and case E includes only GCPs in the block corners (figure 4). With the exception of case A the remaining GCPs were used as a independent check points. The identification and transferring of the GCPs was the most difficult task of the project. The area of interest is hilly with dense canopy and considerable time elapsed of 3 years between the aerial photography mission and the acquisition of the QuickBird images. Illumination, seasonal differences, and view direction imposed other challenges to the operation.

It is important to emphasize that due to the lack of the necessary overlap among individual images for a stereoscopic vision, the results been analyzed are only of horizontal nature. Table 2 summarizes the achieved results based on the ephemeris and quaternion approach using full control distribution (case A).

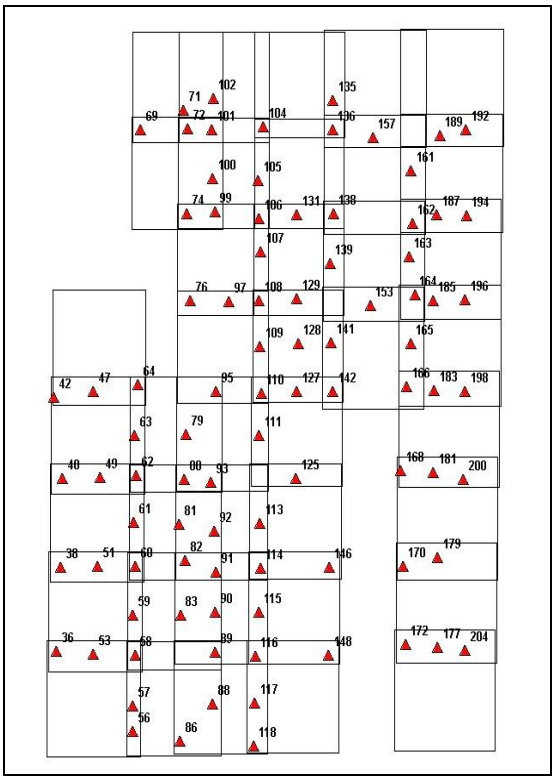

figure 2: control point configuration A

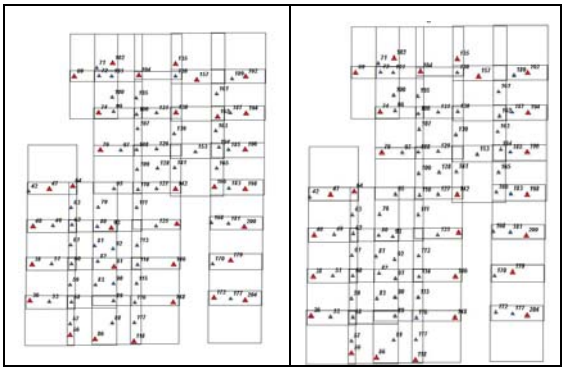

figure 3: control point configuration B left and C right

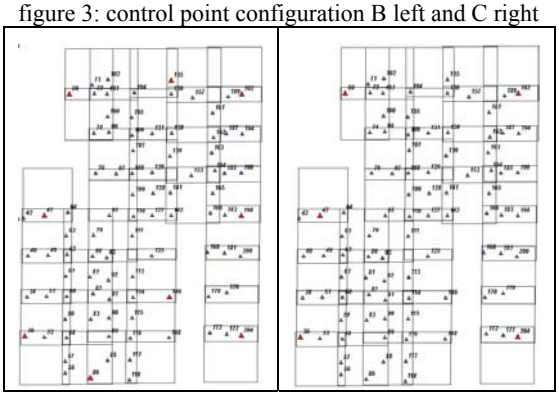

figure 4: control point configuration D left and E right

Case	GCPs	RMSEX [m]	RMSEY [m]
A	89	0.52	0.53
B	33	0.45	0.44
C	25	0.35	0.35
D	9	0.33	0.34
E	5	0.24	0.26

table 2: root mean square discrepancies at control points, orientation based on ephemeris and quaternion approach

Case	check points	RMSEX [m]	RMSEY [m]
A	0	-	-
B	56	1.77	2.59
C	64	1.94	2.72
D	80	3.42	4.21
E	84	5.27	6.93

table 3: root mean square discrepancies at independent check points, orientation based on ephemeris and quaternion approach

From Table 2 one clearly notice that with relaxed control there is a better fitting of the block to the control but the absolute accuracy determined with check points (table 3) deteriorates very quickly reaching non tolerable values for control only in the block corners (case E). Maximal discrepancies at check points of 7.2m for case B, 8.3m for case C, 16.8m for case D and 20.4m for case E appeared.

Case	GCPs	RMSE [m]		Max Errors [m]	
		SX	SY	ΔXmax	ΔYmax
A	89	0.21	0.25	2.53	4.93
B	33	0.19	0.23	2.51	4.56
C	25	0.16	0.22	2.48	1.50
D	9	0.16	0.21	2.45	1.48
E	5	0.15	0.20	2.06	1.35

table 4: internal accuracy of the orientation based on ephemeris and quaternion approach

Table 4 shows the internal accuracy based on statistics on its tie points. It shows a better internal relative fitting between contiguous images for more relaxed control. This is shown in the RMSE and on the maximum residuals. Nevertheless, the reached maximum errors, especially for the full controlled block suggest the presence of not yet detected gross errors among the image observations (i.e., in tie and/or transferred GCPs). In addition it demonstrates the far too optimistic accuracy estimation by the inner accuracy if compared with independent check points.

3.3. Block Adjustment using enhanced Rational Polynomial Coefficients.

Using the same image and the ground control point observations and respecting the same distribution patterns of GCPs and check points as above, the enhanced Rational Polynomial Coefficients model was tested.

Case	GCPs	RMSEX [m]	RMSEY [m]
A	89	0.67	0.71
B	33	0.72	0.79
C	25	0.99	1.01
D	9	1.07	1.15
E	5	1.17	1.22

table 5: : root mean square discrepancies at control points, orientation based on bias corrected RPC

Case	check points	RMSEX [m]	RMSEY [m]
A	0	-	-
B	56	1.22	1.84
C	64	1.88	2.25
D	80	2.71	3.15
E	84	4.02	4.41

table 6: root mean square discrepancies at independent check points, orientation based on bias corrected RPC

From the comparison of tables 2 and 5 we can conclude that for a full ground control distribution (case A) the block adjustment based on the bundle approach (using ephemeredes and quaternion) seems to work better as compared with the enhanced RPC model. Nevertheless, the results from table 6 show a different behavior. In fact shown at independent check points while using the bundle approach with less GCPs, the accuracy is not so good like with the RPC approach. The reason for this difference can be found in the fact that the used QuickBird images do have strong systematic errors, mainly angular affinity. This is removed via the RPCs. In general using the bundle block approach for lesser constraints the systematic errors have the possibility to spread their effects freely over the block. The systematic errors are better modeled and their effects minimized by the use of the bias corrected RPC approach. Nevertheless, one would expect a better performance of the correction functions. This is due to the geometric configuration of the block and the very little overlap between images.

The internal accuracy based on the bias corrected RPC orientation (table 7) like usual shows too small values but a tendency to the correct dependency upon the number of control points like shown at check points. In general it confirms the known meaning of the internal accuracy as far too optimistic, especially for poor control. The unavoidable systematic errors are not respected for the accuracy estimation of internal geometric situation.

Case	GCPs	RMSE [m]		Max Errors [m]	
		SX	SY	ΔXmax	ΔYmax
A	89	0.29	0.32	1.83	2.57
B	33	0.65	0.74	2.01	3.34
C	25	0.81	0.88	2.48	2.25
D	9	0.88	0.97	2.85	2.98
E	5	0.91	1.12	3.08	3.35

table 7: internal accuracy of the orientation based on bias corrected RCP

4. Conclusions

In general QuickBird Basic images do have not modeled systematic errors. Their effect can be removed or at least reduced by self calibration through additional parameters.

Bundle block adjustment of QuickBird Basic imagery simply based on ephemeris and attitude quaternion is not able to account for the effects of systematic errors. Moreover, as any other bundle approach of narrow field of view imagery, with six orientation parameters per image it is not possible to avoid strong correlations between position and attitude. With larger a priority control point standard deviation the block gets less deformed.

Block adjustment based on bias corrected RPCs minimize the effects of the remaining systematic errors of the QuickBird Basic Imagery.

Internal accuracy based on figures of adjusted tie points is more realistic for larger constraints and removal of systematic errors. Care must be taken while analyzing the internal accuracy – it is far too optimistic.

5. Recommendations

To fully test the performance of the above studied block adjustment approaches it is required:

a. Handling of systematic image errors for both methods - the bundle block adjustment based on ephemeris and attitude quaternion as well as bias corrected RPCs.
b. The numerical stability, statistical significance and reliability of each additional parameter for each image has to be tested in order to justify their presence and to avoid over-parameterization.
c. Three dimensional block adjustment shall be carried out using overlapping stereoscopic images. In other words, the images to be used in the block adjustment shall be taken with opposite inclinations within the orbit to allow a real stereo vision.
d. The data shall be free of gross errors. Ground Control and tie/pass points shall be clearly and uniquely visible and determined (the observed large residuals after adjustment of the used data set suggest the presence of at least one blunder).

6. References

Grodecki, J., 2001: Ikonos Stereo Feature Extraction - RPC Approach, ASPRS annual convention, St Louis 2001, on CD

Grodecki, J. and Dial, G. 2003. Block Adjustment of High-Resolution Satellite Images Described by Rational Polynomials. Photogrammetric Engineering and Remote Sensing. Vol. 69, No. 1, January 2003, pp. 59 – 68.

Jacobsen, K., Passini, R., 2003: Comparison of QuickBird and Ikonos images for the generation of Ortho-images, ASPRS Annual Convention, Anchorage, 2003, on CD

Passini, R., Jacobsen, K., 2003: Accuracy of Digital Orthos from High Resolution Space Imagery. Joint Workshop "High Resolution Mapping from the Space 2003", Hannover 2003, on CD + http://www.ipi.uni-hannover.de/

Passini, R., 2004: Digital Orthos Accuracy Study using High Resolution Space Imagery. IT/Public Works URISA Regional Conference. Charlotte, NC 2004

Passini, R., Jacobsen, K. 2004. Accuracy Analysis of Digital Orthophotos from very high Resolution Imagery. IntArchPhRS. volume XXXV, part B4. Istanbul, 2004, pp 695-700

Passini, R., Betzner, D., Jacobsen, K., 2002: Filtering of Digital Elevation Models. ASPRS annual convention, Washington, DC 2002, on CD